

Micro-dystrophin Gene Therapy Partially Enhances Exercise Capacity in Older Adult *mdx* Mice

Buel D. Rodgers,^{1,4} Yemeserach Bishaw,¹ Denali Kagel,¹ Julian N. Ramos,^{2,3} and Joseph W. Maricelli¹

¹School of Molecular Biosciences, Washington Center for Muscle Biology, Washington State University, Pullman, WA 99164, USA; ²Department of Neurology, Senator Paul D. Wellstone Muscular Dystrophy Specialized Research Center, University of Washington, Seattle, WA 98195, USA; ³Molecular and Cellular Biology Program, University of Washington School of Medicine, Seattle, WA, USA

Micro-dystrophin (μ Dys) gene therapeutics can improve striated muscle structure and function in different animal models of Duchenne muscular dystrophy. Most studies, however, used young *mdx* mice that lack a pronounced dystrophic phenotype, short treatment periods, and limited muscle function tests. We, therefore, determined the relative efficacy of two previously described μ Dys gene therapeutics (rAAV6: μ DysH3 and rAAV6: μ Dys5) in 6-month-old *mdx* mice using a 6-month treatment regimen and forced exercise. Forelimb and hindlimb grip strength, metabolic rate (VO_2 max), running efficiency (energy expenditure), and serum creatine kinase levels similarly improved in *mdx* mice treated with either vector. Both vectors produced nearly identical dose-responses in all assays. They also partially prevented the degenerative effects of repeated high-intensity exercise on muscle histology, although none of the metrics examined was restored to normal wild-type levels. Moreover, neither vector had any consistent effect on respiration while exercising. These data together suggest that, although μ Dys gene therapy can improve isolated and systemic muscle function, it may be only partially effective when dystrophinopathies are advanced or when muscle structure is significantly challenged, as with high-intensity exercise. This further suggests that restoring muscle function to near-normal levels will likely require ancillary or combinatorial treatments capable of enhancing muscle strength.

INTRODUCTION

Most muscular dystrophies result from abnormalities in the structure and function of the multi-protein dystrophin-glycoprotein complex.^{1,2} The most common forms, Duchenne and Becker muscular dystrophies (DMD and BMD, respectively), result from genetic anomalies within the X-linked dystrophin gene and, together, occur at an approximate frequency of 1 in every 5,000 male births.^{3,4} The two forms, however, differ in prognosis, which is dependent upon the relative amount of functioning dystrophin protein expressed in striated muscle. Disease progression is rapid and the pathologies are more severe in Duchenne patients who express little to no functioning dystrophin, whereas in Becker patients, truncated dystrophins or low protein levels partially protect striated muscle. Despite these differences, both DMD and

BMD are primarily treated with palliative care and corticosteroids as no currently available treatment can compensate for the loss of functioning dystrophin. Developing treatments include novel gene therapeutics as several preclinical studies very clearly illustrate the corrective potential of adeno-associated viral vectors (AAVs) carrying “micro-dystrophin” (μ Dys) cDNA payload genes.^{5,6}

The approximately 13.9-kb dystrophin cDNA size greatly exceeds the 5-kb packaging capacity of AAVs.^{7,8} Nevertheless, μ Dys, mini-dystrophin, or reconstituted full-length dystrophin cDNAs have proven highly effective in restoring muscle structure and many aspects of muscle function when delivered using an AAV vector.^{5,6} Indeed, three different μ Dys gene therapeutics are currently being developed by Solid Biosciences, Sarepta/Nationwide Children’s Hospital, and Pfizer.⁵ Each therapeutic contains μ Dys cDNA constructs coding for truncated dystrophin proteins that lack several internal repeating motifs. These proteins retain amino- and carboxy-terminal cysteine-rich domains (Figure 1) critical for binding to intracellular γ -actin and to the glycoprotein complex on the muscle cell plasma membrane (i.e., sarcolemma).^{5,6} This provides a functional link between the muscle contractile elements within the cell and the lateral membrane anchoring components, which, in turn, stabilizes the muscle cell and prevents contraction-induced muscle damage and, ultimately, degeneration.^{9,10}

Recent studies compared the efficacy of several novel μ Dys gene therapeutics in *mdx*^{4cv} mice.¹¹ Each μ Dys protein contained functional domains that were either lacking in previously developed versions or that were placed within different intramolecular contexts. They all retained conserved regions for binding to γ -actin and β -dystroglycan and, in addition, contained different combinations of spectrin-like repeats (R1–R24) from the internal rod domain (Figure 1A). Other domains

Received 22 July 2019; accepted 20 November 2019;
<https://doi.org/10.1016/j.omtm.2019.11.015>.

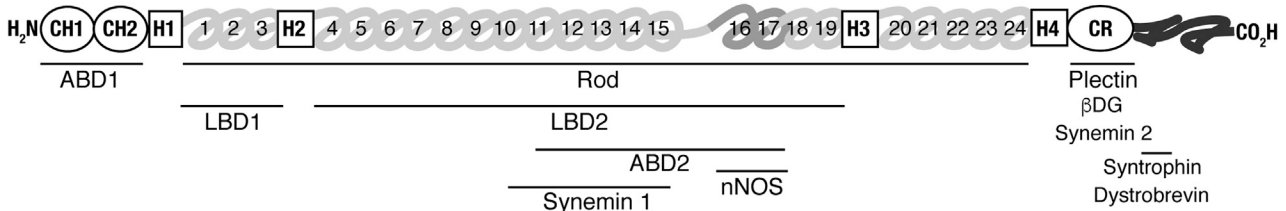
⁴Present address: AAVogen, 13420 Glen Lea Way, Rockville, MD 20850, USA

Correspondence: Buel D. Rodgers, PhD, School of Molecular Biosciences, Washington Center for Muscle Biology, Washington State University, Pullman, WA 99164, USA.

E-mail: danrodders@aavogen.com



A Wild-type dystrophin (427 kDa) & notable structural/binding-domains



B Micro-dystrophin structural compositions

Δ R4-R23/ Δ CT (137 kDa) - Sarepta/Nationwide Children's Hospital



Δ H2-R23/ Δ CT or " μ DysH3" (137 kDa)



Δ R2-R15/R18-R22/ Δ CT or " μ Dys5" (147 kDa) - Solid Biosciences



C Experimental design

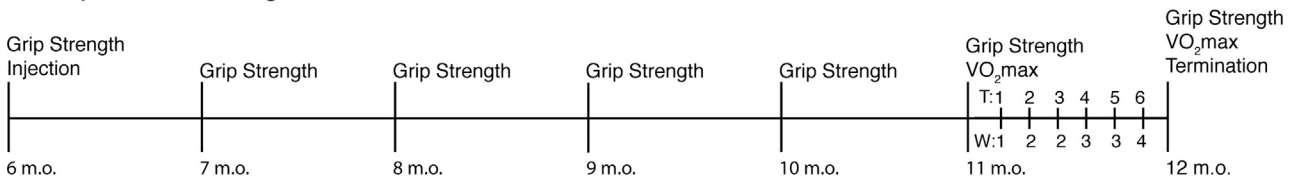


Figure 1. Micro-dystrophin and Experimental Designs

(A) The wild-type dystrophin protein is composed of three general domains: the amino terminus with two calponin homology (CH) domains, the central rod domain composed of spectrin-like repeats (numbered), a cysteine-rich (CR) domain, and a carboxy terminus composed of two coiled-coil repeats.⁶⁸ Other more specific domains are aligned to these and include binding domains for actin (ABD); laminin (LBD); intermediate filaments (synein and plectin); proteins in the DGC complex (β -dystroglycan, syntrophin, and dystrobrevin); neuronal nitric oxide synthase (nNOS), which binds to repeats 16 and 17 via α -syntrophin; and four interspersed hinge domains (H1–H4). Horizontal lines indicate relative positions of labeled domains. (B) Structural components of different micro-dystrophins correspond to those labeled in (A). Also indicated are the mass of each protein and the corporate developer. (C) Treatment timeline of experiments. All mice were 6 months old when starting experiments. Forelimb and hindlimb grip strength measures were collected monthly on all mice, for a total of 7 measures over 6 months. Forced treadmill running was used to assess systemic muscle function and to exacerbate the dystrophic phenotype during the last month. This included initial and final VO₂ max tests and 6 intervening training sessions (T1–T6) over 4 weeks (W1–W4). Mice were terminated 24 h following the last VO₂ max test. Procedures are listed above the timeline, and ages of mice are listed below.

were incorporated and included two or three of the hinge domains (H1–H4) that contribute to protein flexibility. Repeats R16–R17 were also included as they are necessary for neural nitric oxide synthase (nNOS) localization to the dystrophin glycoprotein complex at the sarcolemma.^{12–14} One of the constructs tested here, μ DysH3, is structurally similar to that being developed by Sarepta/Nationwide Children's Hospital (ClinicalTrials.gov: NCT03375164) and differs only by a switched hinge domain, H3 for H2.¹⁵ Unlike μ Dys5, which is being developed by Solid Biosciences (SGT-001; ClinicalTrials.gov: NCT03368742), neither of these constructs contain R16 and R17 (Figure 1B). Thus, it is possible that they provide more flexibility due to the additional hinge domain but lack an nNOS binding domain that can preserve contraction-induced vasodilation, thereby preventing ischemic damage.¹² Both μ DysH3 and μ Dys5, however, lack H2 and should not produce a ringbinden phenotype.^{15,16}

These recent studies suggest that refinements to the rod domain alone can significantly improve the functionality of μ Dys gene therapeutics when compared to the previously established "best" candidate, μ DysH3.¹¹ They identified two constructs that performed slightly better than the others and this includes μ Dys5. However, these studies were performed using very young mice (2 weeks old), as do most pre-clinical studies for DMD, and only minimal tests of muscle function (specific force and contraction-induced injury). Such assessments are highly appropriate for establishing proof of concept and for comparing the relative efficacy of different therapeutics, but their results may not translate to clinical success as the development of pathophysiological signs in any dystrophic model accumulates with age. More comprehensive studies of older dystrophic mice using rigorous tests of muscle function are, therefore, needed to adequately determine the relative effectiveness of any treatment.

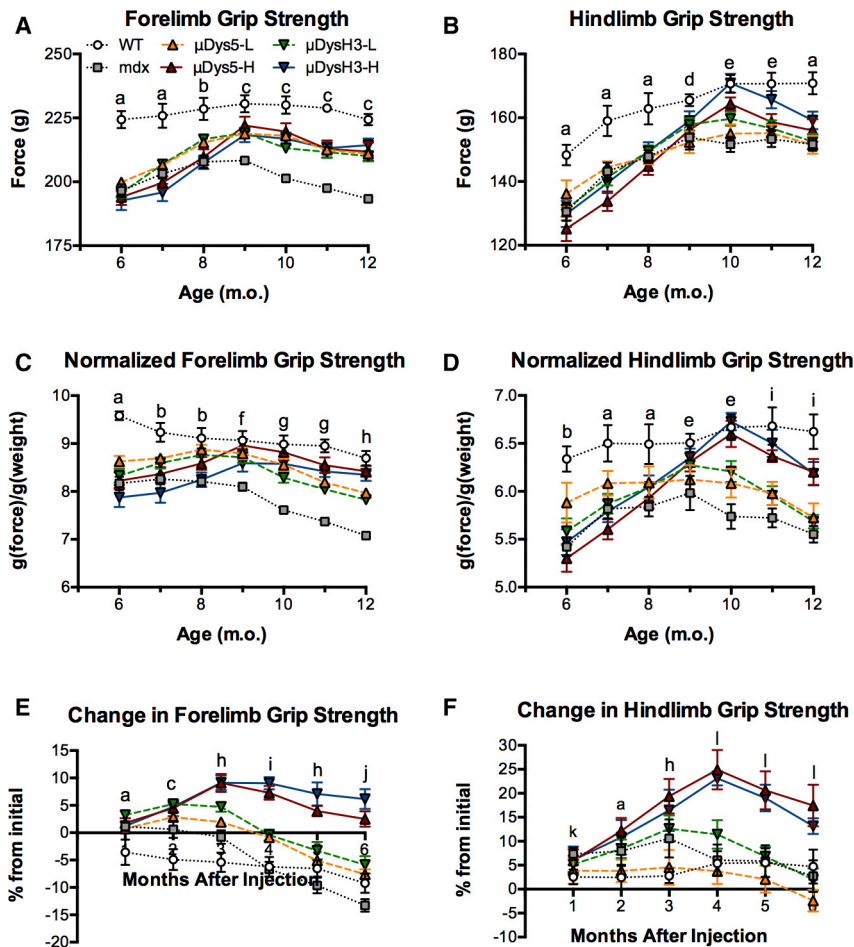


Figure 2. Changes in Forelimb and Hindlimb Grip Strength over Time

Mice were injected with 0 , 5×10^{11} (low dose, -L), or 5×10^{12} (high dose, -H) vg of rAAV6: μ Dys5 (μ Dys5) or rAAV6: μ DysH3 (μ DysH3), and grip strength was measured monthly as in Figure 1. The key in (A) applies to the whole figure and each point represents mean \pm SEM ($n = 6$, $p \leq 0.05$). (A–D) Absolute forelimb (A), absolute hindlimb (B), normalized forelimb (C), and normalized hindlimb (by body weight) grip strength of wild-type (WT, injected with 0 vg) C57BL/10 and *mdx* mice injected with all doses (*mdx* = 0 vg). (E and F) Percent change in absolute forelimb (E) and hindlimb (F) grip strength from the initial measurements (time 0). The only difference between vectors occurred in (B) (μ DysH3-H > μ Dys5-H) at 10 and 11 months. Otherwise, significant differences between dose groups are indicated by letters as follows: a, WT differs from all other groups; b, WT differs from all others, and low doses differ from high and *mdx*; c, WT differs from others, and both doses differ from *mdx*; d, WT differs from low doses and *mdx*, while both doses differ from *mdx*; e, WT differs from low doses and *mdx*, while both doses differ from *mdx*; f, *mdx* differs from all others; g, WT and high doses differ from others, and low doses differ from *mdx*; h, the dose groups, WT, and *mdx* all differ from each other; i, high and low doses both differ from all others; j, high doses and *mdx* differ from others; k, no differences; l, high doses differ from others.

We compared μ DysH3 and μ Dys5 gene therapeutics using older adult *mdx* mice and chronic exercise exacerbation as this produces a dystrophic phenotype that more closely resembles the human condition.^{17–21} Our experimental design incorporated a long treatment period of 6 months and tests of systemic muscle function that resemble those used in clinical trials (e.g., 6-minute walk test, respiratory function, grip strength). Our results indicate that both therapeutics possess the potential to significantly improve different aspects of skeletal muscle structure and systemic muscle function, even when the dystrophinopathies are advanced. Nevertheless, they also indicate that both therapeutics were only partially effective at the doses tested. This is consistent with previous studies using old *mdx* mice,^{22–25} often with even higher doses of similar μ Dys gene therapeutics, and suggests that ancillary support may be needed to compensate for the accumulated effects of muscle degeneration over time.

RESULTS

Study Design

Experiments were performed on untreated wild-type C57BL/10 control mice and on treated and untreated *mdx* mice. Mice were first analyzed and treated when 6 months old and were terminated when 12 months old (Figure 1C). Compared to young adult *mdx*

mice (e.g., 2–3 months old), such older adult mice express a more pronounced dystrophic phenotype but are still capable of completing rigorous exercise protocols.^{19,21} Grip strength measures were collected on all mice before injecting the treated groups, which received retro-orbital (RO) injections of low (5×10^{11} vg per mouse) or high (5×10^{12} vg per mouse) doses of rAAV6: μ Dys5 or rAAV6: μ DysH3 immediately after assessing initial fore- and hindlimb grip strength. Such measures were subsequently collected monthly for 6 additional months. During the final month, mice exercised twice weekly on respiratory treadmills, with 2 and 3 days of rest between exercise sessions, using a previously optimized protocol for assessing systemic muscle function in *mdx* mice.²⁰ This included initial and final VO_2 max tests, which measures the maximal volume of O_2 consumed during exercise, on weeks 1 and 8 and six intervening “training” sessions. Final grip strength measures were collected immediately before the last VO_2 max test, and mice were subsequently terminated after 24 hr.

Grip Strength

When the study began, absolute forelimb and hindlimb grip strength of wild-type mice was significantly higher than that of all *mdx* mice, regardless of treatment group (Figures 2A and 2B). The forelimb levels remained relatively constant in wild-type mice thereafter, increased and plateaued in treated mice, and steadily declined in untreated *mdx* mice after 3 months. No differences were detected among the treated groups, although their values were significantly higher than those of untreated *mdx* mice and lower than those of

Table 1. Change in Body Mass

	WT	Mdx	μ Dys5-L	μ Dys5-H	μ DysH3-L	μ DysH3-H
Initial	23.4 \pm 0.3	24.0 \pm 0.2	23.2 \pm 0.3	23.2 \pm 0.3	23.5 \pm 0.3	24.2 \pm 0.2
Final	25.8 \pm 0.3	27.3 \pm 0.2	26.5 \pm 0.3	25.2 \pm 0.3	26.8 \pm 0.3	25.7 \pm 0.2
% change	10.3 \pm 0.1	13.5 \pm 0.2	14.3 \pm 0.3	6.6 \pm 0.3	14.1 \pm 0.3	6.3 \pm 0.1

wild-type mice at several time points, especially at and after 3 months. Normalizing the forelimb data to body mass helped distinguish differences between high and low doses, but not between vectors, as the high doses of both vectors restored strength to wild-type levels, while the low doses only partially restored strength (Figure 2C).

Normalizing these data to body mass is somewhat misleading as the body composition and mass of older wild-type and *mdx* mice often differ and can change disproportionately (Table 1). In fact, the similarities in forelimb grip strength among wild-type mice and *mdx* mice treated with high doses of either vector are due, in part, to normalization, as the body mass of the former increased by approximately 10% and that of the latter increased by 6%. This suggests that treating mice with high vector doses enhanced, but did not completely restore, forelimb strength to normal. Tracking relative changes of normalized forelimb grip strength over time further distinguished the high-dose groups from all the others (Figure 2E). Indeed, strength increased and was maintained in these mice, although there was a net decrease in the other groups.

Over the first 4 months, absolute hindlimb grip strength steadily increased in all groups (Figure 2B), which typically occurs in our experience as mice slowly become accustomed to the assay. Normalizing grip strength identified differences similar to those of the forelimb measures, as again, no differences were detected between the vectors and the low-dose treatment had no significant effect while the high doses progressively increased strength. Moreover, high-dose treatment fully restored strength in 4 months, although it declined significantly thereafter, a pattern that also occurred when plotting relative changes (Figures 2D and 2F). The latter results are possibly the most informative and very clearly indicate greater responsiveness among the high-dose groups, despite the fact that both fore- and hindlimb grip strength began to decline after 3 or 4 months, even in these groups. Nevertheless, as a whole, the grip strength results together suggest that high doses of either vector are needed to have long-term effects on partially restoring grip strength, at least in this particular (i.e., aged) dystrophic mouse model.

Exercise Capacity

The initial VO_2 max of all *mdx* mice, treated or not, was significantly lower than that of wild-type mice (Figure 3A). Five months of μ Dys gene therapy was, therefore, incapable of maintaining VO_2 max in 11-month-old mice. Due to the older age of mice when the exercise protocol began, the VO_2 max of most mice, including wild-type mice, decreased from initial to final tests. This was not unexpected as

improved VO_2 max only occurs with repeated high-intensity interval training and has not been demonstrated in wild-type or *mdx* mice using the protocol described herein.^{20,26,27} However, the initial and final VO_2 max values were not significantly different in *mdx* mice receiving high-dose vector treatment. Note that the relative change in VO_2 max among these groups was nearly identical to that of wild-type mice, just one third, and significantly different from the change in untreated *mdx* mice (Figure 3B). These results are highly novel and suggest that, even in older *mdx* mice, high-dose vector treatment can prevent the deleterious effects of exercise-induced muscle damage and preserve maximal exercise capacity as measured by VO_2 max. The differences in total distance traveled (Figures 3C and 3D) resembled those of VO_2 max, and although many were not significant, the overall similar pattern further highlights the beneficial effects of μ Dys gene therapy on exercise performance.

The reduced exercise capacity among all *mdx* mice is possibly best illustrated by the total energy expended during the initial VO_2 max test (Figure 3E). In fact, there were no differences in the total energy expended among the groups, despite the fact that treated and untreated *mdx* mice ran shorter distances. In the final VO_2 max test, the energy expended was lower in all but wild-type mice (Figures 3E and 3F). This was consistent with mice running shorter distances except in mice receiving high doses of either vector where, in comparison to the other groups, the relationship between distance traveled and energy expended were inversely correlated. These mice ran similar or longer distances than the others but expended fewer calories (Figure 3G). This is best illustrated by the energy expenditure rate, an inverse measure of running efficiency, which increased in all groups between tests except in *mdx* mice treated with high doses. Indeed, the rate decreased by 13% and 20% in mice treated with rAAV6: μ Dys5-H and rAAV6: μ DysH3-H, respectively (Figure 3H). This indicates that high-dose treatment of either vector improved running efficiency as mice ran farther while consuming less energy.

Exercise Training

Previous studies identified pathological markers of exercise training in the *mdx* mouse and in the P448L mouse, a model for limb girdle muscular dystrophy 2i.^{20,28} The markers include motivational shock accumulation, VO_2 cv (VO_2 coefficient of variation, a measure of VO_2 variability during exercise), minimum VO_2 , and maximum respiratory exchange ratio. Throughout the 4-week period, the number of accumulated shocks increased in all groups. The rate of increase was not equal, however, as the final number in *mdx* mice treated with no or low-dose vectors was 4-fold higher than that of wild-type mice (Figure 4A). Most importantly, treating *mdx* mice with high doses of either vector significantly reduced shock numbers compared to these groups, although shock levels remained 3-fold higher than those in wild-type mice.

This pattern of responsiveness is similar to the patterns previously discussed where treating with high vector doses improves but does not restore muscle function, although other aspects of exercise training were, for the most part, unaffected by any treatment. This

includes the respiratory metrics as well as total energy expended (Figures 4B–4F). In fact, very few differences were noted regardless of metric, training session, or group comparison. This differs from our previous studies of young dystrophic mice where all of these metrics differed between dystrophic and wild-type mice, suggesting that advanced age is itself a confounding factor. Nevertheless, both doses of both vectors partially restored VO_2 cv for the entire study period as values for treated *mdx* mice were different from both wild-type and untreated *mdx* mice (Figure 4B).

Histological Analysis and Serum Creatine Kinase (CK)

Ramos et al.¹¹ previously demonstrated rAAV6:μDys5 to reduce muscle fibrosis and both rAAV6:μDys5 and rAAV6:μDysH3 to be equally effective in transducing muscle μDys expression and in reducing other aspects of muscle structure and function over a 6-month treatment period, the same period used in the present study. We, therefore, quantified differences in central nuclei, as this is a more acute metric of muscle regeneration. Skeletal muscle injury, either from normal exercise or from pathological insult, induces satellite cell nuclei incorporation into regenerating fibers. The presence of central nuclei is, therefore, a well-established degenerative and regenerative marker in dystrophic muscle. Although total nuclei counts were similar in all groups, several significant and tissue-specific differences in central nucleation were detected (Figures 5A–5C). This was especially apparent in tibialis anterior (TA) and gastrocnemius muscles where the percentage of fibers with central nuclei as well as the number of central nuclei were elevated in *mdx* compared to those in wild-type mice (Figures 5B and 5C). Moreover, both vectors reduced these metrics by 33%–50% and in a dose-dependent manner, although neither vector fully restored wild-type levels. By contrast, quadriceps and diaphragm were mostly unresponsive to treatment at these doses as only the high dose of rAAV6:μDys5 had a significant effect in these specific muscles.

Muscle degeneration is also associated with muscle atrophy and with reductions in the average muscle fiber cross-sectional area. In fact, the relative number of small muscle fibers in *mdx* mice was 2- to 3-fold higher than in wild-type mice, while conversely, the number of large fibers was only 33%–50% of wild-type counts (Figures 5E–5G). This was true for all muscles examined. High doses of either vector altered the fiber size distribution pattern toward wild-type (i.e., fewer small fibers and more medium or large fibers), with the greatest effect occurring in TA muscles, which were almost fully restored. The high vector doses also reduced serum CK levels, a circulating marker of muscle degeneration, by over 60% (Figure 5H). These data are consistent with the functional data presented and, again, suggest that moderately high doses of rAAV6:μDys5 or rAAV6:μDysH3 can significantly improve a severe dystrophic phenotype—in this case, using muscle structure as an endpoint—but may not be able to restore it.

DISCUSSION

Because the dystrophic phenotype in *mdx* mice progressively develops,^{18,19,21} many pathologies commonly expressed even in young DMD patients are not expressed in young *mdx* mice (fibrosis, muscle

hypertrophy, cardiac dysfunction, etc.). Thus, the older *mdx* mouse is, in many ways, a superior preclinical model to the more commonly used young *mdx* mouse. Early expression of disease pathologies can also be induced with high-intensity exercise.^{17,29–31} In fact, the TREAT-Neuromuscular Disease (TREAT-NMD) network recommends using exercise as a quantitative endpoint in preclinical studies with *mdx* mice.³² TREAT-NMD also provides several standardized protocols for testing *mdx* mice, including forced exercise and quantifying respiratory and exercise performance.^{20,33–35} Our combined use of older *mdx* mice and forced treadmill running, therefore, represents a rigorous attempt to accurately represent a more clinically relevant condition where muscle structure and function are compromised from the accumulated effects of muscle degeneration.

Both gene therapeutics tested significantly enhanced various aspects of skeletal muscle structure and function, although the low doses tested had minimal significant effects on just a few variables quantified (e.g., grip strength at some time points, measures of muscle size in some muscles, VO_2 cv). By contrast, the high doses were effective overall at enhancing or preserving measures of grip strength and exercise capacity (e.g., VO_2 max, distance traveled, metabolic rate, shock accumulation) while also preserving muscle fiber size and preventing some degeneration (i.e., central nucleation). This protectiveness, however, was only partially effective, as none of the metrics measured was restored to healthy wild-type levels at the doses used here, which has been previously noted in other studies using aged *mdx* mice.^{22–25}

Gregorevic et al.²² treated 20-month-old *mdx* mice for 4 months with 1×10^{13} vg of a “first-generation” μDys vector and reported partial effectiveness. The specific μDys expressed in this study (ΔR4-23/ΔCT; Figure 1B) is structurally similar to μDysH3 but contains H2 instead of H3. It also similarly restores some muscle function in side-by-side comparisons, although animal studies indicate that it can produce ringed fibers with contraction-induced injury.¹⁵ Gregorevic et al.²² reported that the body mass of treated *mdx* mice was slightly higher than that of untreated *mdx* mice and was restored to only 50% of wild-type levels. Serum CK levels were substantially reduced but remained elevated. The fiber size distribution, central nucleation, and specific force of TA or diaphragm muscles were either not affected by the treatment or were only minimally affected, and although treated diaphragms were protected from contraction-induced injury, TA muscles were not.

Gregorevic et al.²² administered a suboptimal dose (producing fewer than 100% transduced fibers) that is 2-fold higher than the highest dose used herein, yet they also reported partial restoration of muscle structure and function. Partial restoration of the cardiac phenotype in aged *mdx* mice was also reported using 5×10^{12} vg of a cardiac-optimized μDys and AAV9 serotype vector.^{23,24} This is contrasted by earlier studies with young mice where a more complete restoration was demonstrated.³⁶ Wasala et al.³⁷ recently reported that the cardiac-specific overexpression of a mini-dystrophin in 22-month-old transgenic *mdx* mice normalized ECG abnormalities and improved

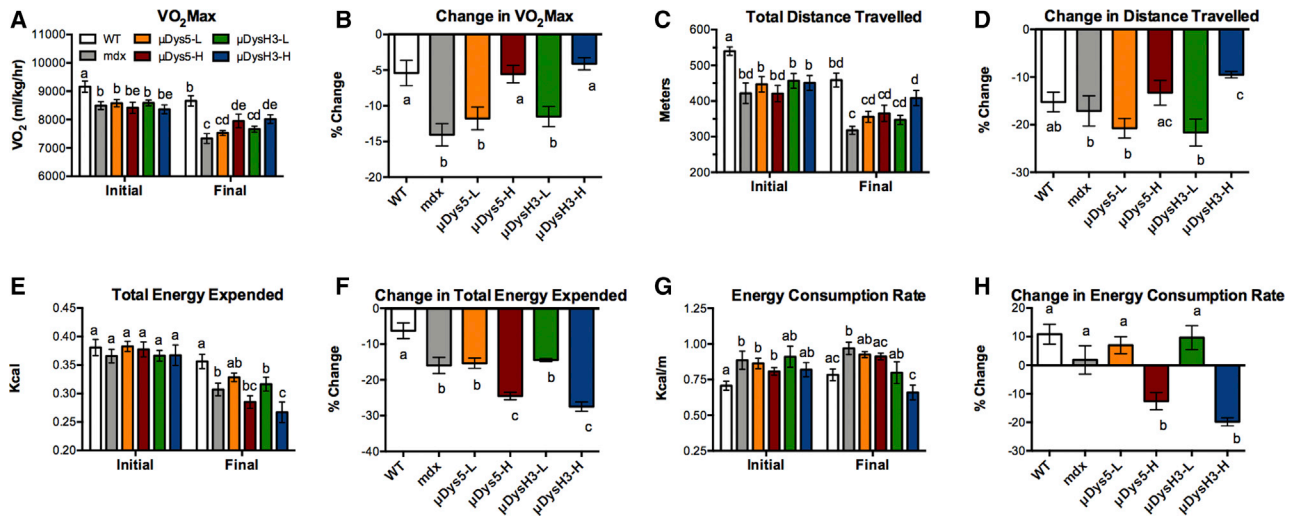


Figure 3. Metrics of Exercise Capacity

VO_2 max tests were performed on wild-type (WT) and *mdx* mice, 5 (initial) and 6 (final) months after injecting with $0, 5 \times 10^{11}$ (low dose, -L), or 5×10^{12} (high dose, -H) vg of rAAV6: μ Dys5 (μ Dys5) or rAAV6: μ DysH3 (μ DysH3) (see Figure 1). WT and *mdx* mice were injected with 0 vg, the key in (A) applies to the whole figure, and each histogram bar represents mean \pm SEM ($n = 4-6$). (A and B) VO_2 max (A) and the change from initial to final (B). (C and D) Distance traveled before mice fatigued (C) and the change from initial to final (D). (E and F) Indirect calorimetry was used to calculate the total energy expended (E) and the change from initial to final (F). (G and H) The energy consumption rate was then calculated by normalizing energy expenditure values to total distance traveled (G) and the change in the energy consumption rate (H). Significant differences between any two groups ($p \leq 0.05$) are indicated by different letters, whereas shared letters indicate no difference.

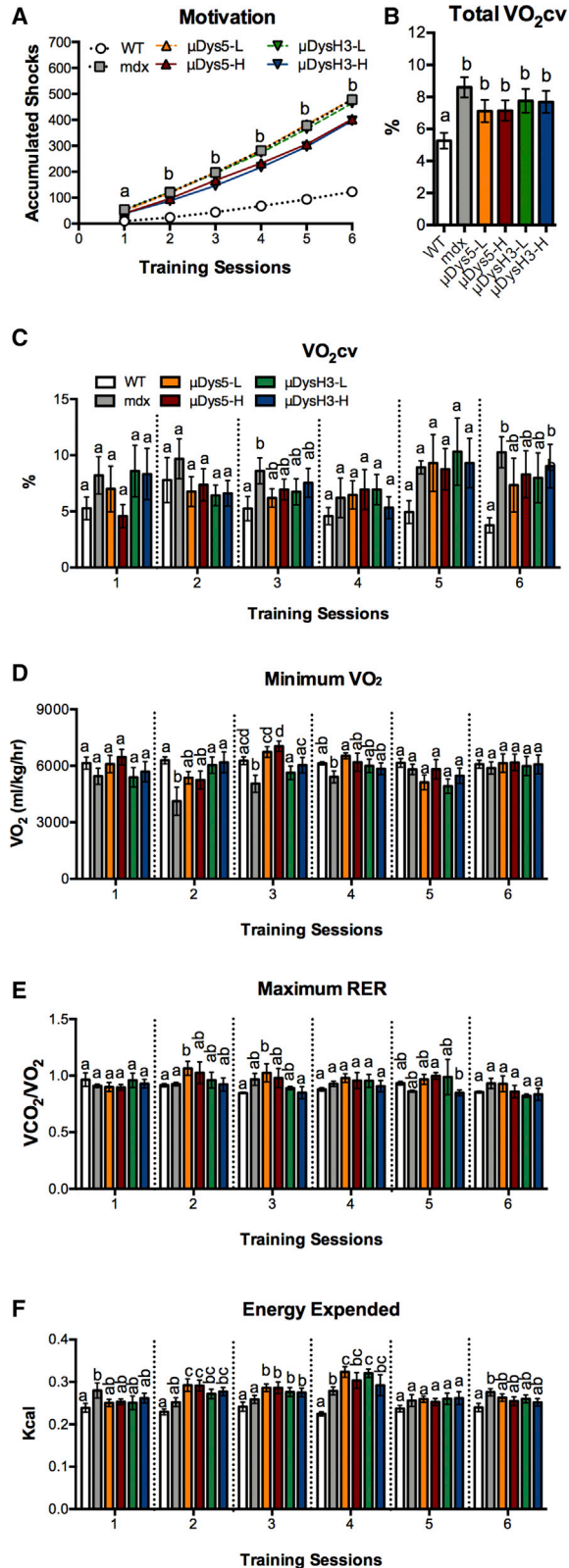
cardiac hemodynamics, despite the fact that heart rate, QRS interval, and Q wave amplitude were only partially corrected. Furthermore, hemodynamics were improved, but far from normalized, and the hearts themselves were hypertrophic.

All of this together suggests that the partial amelioration of dystrophic pathologies in older *mdx* mice is actually the norm at medium to high vector doses. It even occurs in many preclinical studies with young *mdx* mice, further indicating that ancillary treatments are needed to maximize the corrective potential of replacement gene therapy for muscular dystrophy. This is particularly true when using a rigorous model system like older mice and exercise-induced injury that more closely mimic the clinical condition where the accumulated impact of disease pathogenesis (e.g., fibrosis, inflammation, and necrosis) compromises not only muscle function, but also its maximum functional potential. Emerging from this “degenerative hole” would presumably require the development of new and healthy fibers or, alternatively, substantial enhancement to many of the remaining fibers.

Ancillary or combinatorial approaches that complement μ Dys gene therapeutics are hardly novel as previous studies clearly demonstrated the benefit of co-delivering a muscle growth promoter, like follistatin or insulin-like growth factor 1 (IGF1), along with μ Dys in *mdx* mice.³⁸⁻⁴⁰ In fact, an AAV-based follistatin gene therapeutic has already been tested in phase I and phase IIa clinical trials as a sole treatment for BMD.⁴¹ Follistatin binds and antagonizes ActRIIb ligands, including myostatin, GDF11, and activin,⁴² and successfully improved muscle function in these trials. It also improved muscle

function in preclinical proof-of-concept studies with *mdx* mice,⁴³⁻⁴⁸ and its use as a co-therapeutic is superior to that of μ Dys gene therapy alone.⁴⁰ These latter studies demonstrated complete restoration of skeletal-muscle-specific force and resistance to contraction-induced injury in 23-month-old *mdx* mice, whereas μ Dys gene therapy alone had minimal effects. However, follistatin’s promiscuity for multiple ActRIIb ligands requires it to be administered intramuscularly, as targeting the ligands in circulation via any number of approaches (immunoneutralization, ligand traps, follistatin, etc.) has the potential to produce very serious off-target effects or to be less effective.⁴⁹⁻⁵¹ By contrast, we recently developed a Smad7 gene therapeutic (AVGN7) that attenuates the intracellular signaling pathways of ActRIIb receptors in striated muscle and, as a result, avoids these off-target effects and enhances striated muscle mass and function as well as exercise and cardiac capacity.^{52,53} Future studies will, therefore, evaluate the efficacy of a combinatorial approach that co-delivers AVGN7 with one of the μ Dys vectors described herein.

Both rAAV6: μ Dys5 and rAAV6: μ DysH3 proved to be similarly effective in nearly all of the assessments. This was not entirely unexpected, as although μ Dys5 was one of the two top-performing micro-dystrophins tested in a recent comparison by Ramos et al.,¹¹ it was not able to produce a full functional correction. It did, however, localize nNOS to the sarcolemma, and although physiological responses to this were not directly measured, other studies indicate that ischemia and edema are prevented by such actions.^{12,54} Ramos et al.¹¹ also reported that gastrocnemius-specific force was similar in mice treated with rAAV6: μ Dys5 or rAAV6: μ DysH3, while resistance to contraction-induced injury was virtually identical whether gastrocnemius or

**Figure 4. Metrics of Exercise Training**

Wild-type (WT) and *mdx* mice were injected with 0, 5×10^{11} (low dose, -L), or 5×10^{12} (high dose, -H) vg of rAAV6:μDys5 (μDys5) or rAAV6:μDysH3 (μDysH3). WT and “*mdx*” mice were injected with 0 vg, the key in (A) applies to the whole figure, and each histogram bar represents mean \pm SEM (n = 6). Between the two VO₂ max tests, mice trained on respiratory treadmills twice a week for 6 sessions, with sub-maximal effort, at the same speed and time while respiratory gas exchange was continuously monitored. (A) Electrical shocks are used to encourage mice to remain on the treadmill and their quantification is a metric of motivation. Differences between groups are as follows: a, none; b, WT < high doses < low dose = *mdx*. (B and C) The fluctuating respiratory pattern common to dystrophic mice²⁰ was quantified by calculating the mean VO₂ coefficient of variation for (B) the entire training period or (C) each session. (D and E) This fluctuating pattern often results in lower (D) minimum VO₂ and higher (E) maximum respiratory exchange ratio (RER). (F) Total energy expended during each session was calculated using indirect calorimetry. In (B)–(F), significant differences ($p \leq 0.05$) between any two groups are indicated by different letters; shared letters indicate no difference.

diaphragm muscles were used. In addition, Ramos et al.¹¹ treated 2-week-old *mdx*^{4cv} mice with 1×10^{13} vg per mouse, whereas we treated 24-week-old *mdx* mice with half as much vector. Although *mdx*^{4cv} mice express a more severe phenotype at an earlier age, the older *mdx* mice were likely more debilitated, especially as exercise was used to exacerbate the phenotype. Thus, the similar responsiveness to rAAV6:μDysH3 and rAAV6:μDys5 in the present study could be explained by the use of animals that are more severely debilitated as well as the use of relatively lower vector doses; the challenge was simply too significant to distinguish subtle differences in efficacy.

Because cardiac and respiratory failure is ultimately responsible for morbidity and mortality among DMD patients,^{55,56} the significant effects of high-dose vector treatment on metrics of exercise capacity, especially VO₂ max and energy expenditure rate, are particularly important. Indeed, changes in these factors are primarily influenced by cardiac rather than skeletal muscle function, unless the former has been optimized with training,⁵⁷ which did not occur in the present study and, according to our previous study, is unlikely to occur even in young *mdx* mice.²⁰ This suggests that both μDys gene therapeutics have the potential to address the primary cause of death in DMD patients. It also suggests that the non-significant differences between rAAV6:μDys5 and rAAV6:μDysH3 could have practical consequences, although such reasoning naturally assumes that the treatment efficacy described for mice will translate in clinical trials.

The clinical success of DMD therapeutics may very well depend upon their ability to ameliorate advanced pathologies as the disease is typically diagnosed well after many disease symptoms are noticed. Patients are historically diagnosed at the average age of 5 years, although some are diagnosed much later even in their mid-20s.^{4,58} Furthermore, the delay between the expression of early stage pathologies (lethargy, weakness, hypertrophied calf muscles, etc.) and official diagnosis is often many years,^{58–60} during which the disease progression worsens. All of this suggests that proof-of-concept studies of μDys gene therapeutics with older *mdx* mice may be more predictive of clinical success than those using young mouse models. Such reasoning applies to other disease interventions (different μDys

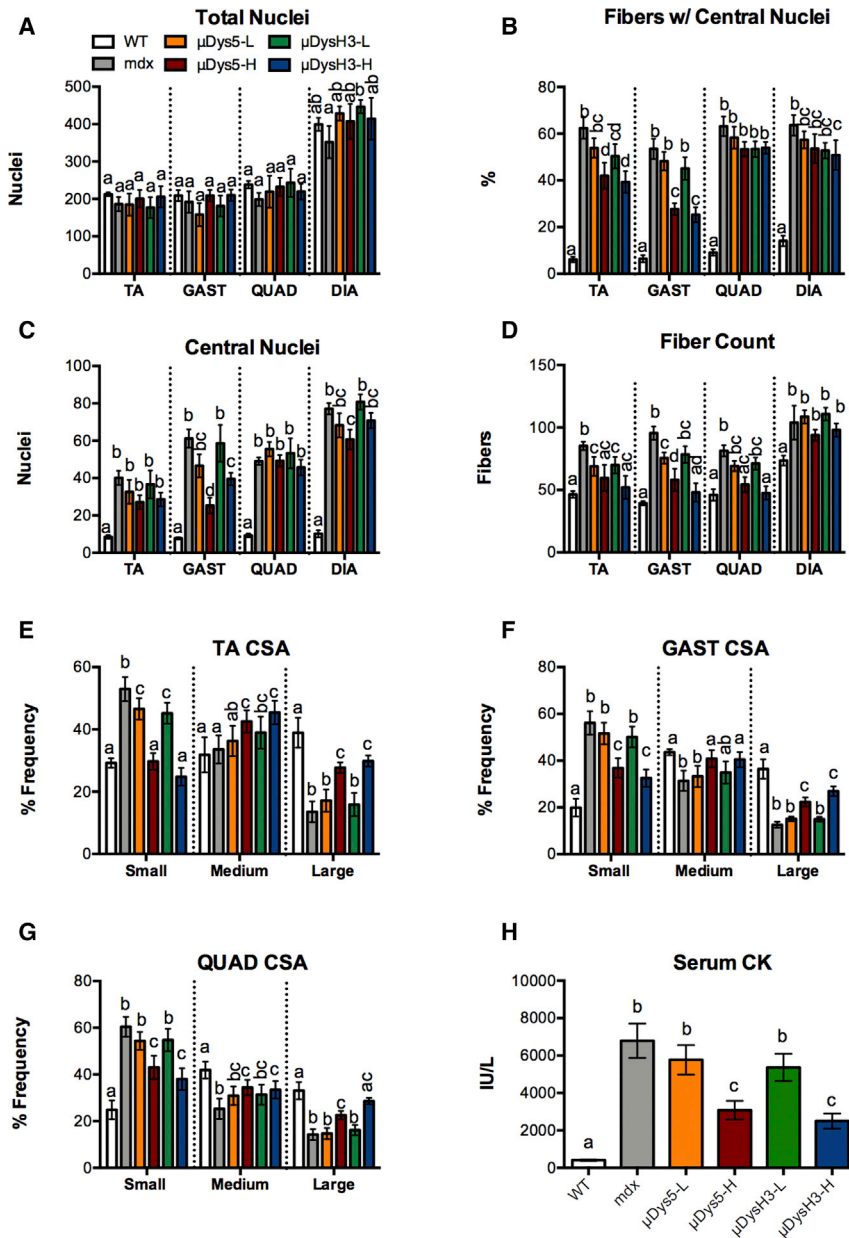


Figure 5. Histopathological Metrics

(A–D) Fiber and nuclei counts per field in different skeletal muscles (TA, tibialis anterior; GAST, gastrocnemius; QUAD quadriceps; and DIA, diaphragm) of wild-type (WT) and *mdx* mice injected with $0, 5 \times 10^{11}$ (low dose, -L), or 5×10^{12} (high dose, -H) vg of rAAV6: μ Dys5 (μ Dys5) or rAAV6: μ DysH3 (μ DysH3). (A) Total nuclei. (B) Fibers with central nuclei. (C) Central nuclei. (D) Fiber count. WT and “*mdx*” mice were injected with 0 vg, the key in (A) applies to the whole figure, and each histogram bar represents mean \pm SEM (n = 4–6). (E–G) Fiber cross-sectional area (CSA) of (E) TA, (F) GAST, and (G) QUAD muscles parsed by fiber size groups: <3,000 μ m, small; 3,001–7,000 μ m, medium; and >7,000 μ m, large. (H) Mice were sacrificed, and serum was collected 24 h after the final VO_2 max test to quantify serum CK levels. Significant differences ($p \leq 0.05$) between any two groups are indicated by different letters, whereas shared letters indicate no difference.

cassette,^{61–67} cDNA expression constructs for μ Dys5 and μ DysH3, and flanking AAV serotype 2 inverted terminal repeats was constructed using standard recombinant methodology. The resulting plasmids, pAAV-CK8- μ Dys5 and pAAV6-CK8- μ DysH3, were then used to co-transfect HEK293 cells with pDGM6 packaging plasmids. Recombinant vectors were subsequently purified from conditioned medium using ion exchange and heparin chromatography followed by CsCl gradient centrifugation to remove empty AAV6 capsids. Concentrated stocks of vector were then suspended in PBS and stored at -80°C until use.

Animal Care

Breeding colonies of wild-type C57BL/10 and dystrophic *mdx* mice were maintained in environmentally controlled rooms of an accredited vivarium, under a 12-h:12-h light:dark cycle at Washington State University. Male mice were provided food and water *ad libitum* and were randomly assigned to treated and untreated

gene therapeutics, gene editing, exon skipping, etc.) as well. It also supports the use of ancillary approaches to enhance dystrophic muscle function, as no therapy to date has ever restored dystrophic muscle function to non-diseased levels.

MATERIALS AND METHODS

Vector Construction

The recombinant AAV6 μ Dys vectors reported herein were prepared in the vector core of the Sen. Paul D. Wellstone Muscular Dystrophy Specialized Research Center at the University of Washington, as previously described.¹¹ Briefly, a custom AAV transfer plasmid containing the previously described muscle-specific CK8 regulator

groups (n = 6) when 6 months old. Maintenance and use of these mice was performed according to a protocol preapproved by an institutional animal care and use committee that met all requirements specified by the Guide for the Care and Use of Laboratory Animals. Prior to treatment, forelimb and hindlimb grip strength measures were recorded for 6-month-old mice as described later. The *mdx* mice were then anesthetized via an intraperitoneal (i.p.) injection of 0.25 mg/g tribromoethanol (Avertin) and subsequently injected retro-orbitally with 5×10^{11} vg ($2\text{--}2.2 \times 10^{13}$ vg/kg body mass) or 5×10^{12} vg ($2\text{--}2.2 \times 10^{14}$ vg/kg) rAAV6: μ Dys5 or rAAV6: μ DysH3 in a total volume of 150 μ L sterile PBS. These doses have been extensively used and were chosen to help distinguish differences between

vectors, as the use of sub-optimal doses—those that do not transduce 100% of the fibers—are more likely to identify differences between vectors when assays that produce sigmoidal response curves are used. Additional groups of untreated wild-type and *mdx* mice were also included as controls.

Grip Strength

Grip strength was quantified on a monthly basis using the Columbus Instruments Grip Strength Meter (Columbus, OH, USA). Forelimb measurements were collected by gently pulling the mouse backward by the tail until the front paws released the T-bar attachment. A mesh attachment was used for collecting hindlimb measurements. Mice were scruffed, hindpaws were raked across the mesh, and then grip strength was again recorded during the release. For both assays, grip measurements were replicated 5 times each session, with intervals at a minimum of 1 min between replicates. This ensures accuracy, reduces variability, and prevents habituation. Mean values were calculated for each mouse at each time point. These values were then used to create in-group replicates.

Forced Treadmill Exercise

A four-lane OxyMax FAST Modular Treadmill System from Columbus Instruments (Columbus, OH) was used to quantify different metrics of exercise capacity and respiration using a protocol optimized for *mdx* mice as previously described.²⁰ Motivational shock units were programmed to administer a 0.65-mA shock for 200 ms at a frequency of 1 Hz, and airflow through the treadmill chambers was set at a rate of 0.6 L/min. Mice were acclimated to treadmills by walking at 5 m/min for 5 min on 3 consecutive days. Mice then began exercise training with an initial VO_2 max test that was followed by 6 training sessions and a final VO_2 max test (Figure 1C).

Both VO_2 max tests were performed at a 25° incline. Mice ran 5-min intervals of 5, 9, 12, and 15 m/min. The treadmill speed then increased 1.8 m/min every 2 min until mice reached exhaustion (i.e., failure to reengage the treadmill for 10 consecutive seconds). When this occurred for a particular mouse, the shock unit was deactivated. VO_2 max was confirmed by the respiratory exchange ratio (RER) approaching 1.1 and a concurrent VO_2 peak. Caloric expenditure was calculated using $\text{CV} = 3.815 + 1.232 \cdot \text{RER}$, which was derived from the linear positive correlation between heat per liter of O_2 (in kilocalories). This, in turn, was calculated using $\text{heat} = \text{CV} \cdot \text{VO}_2$, RER, and total energy expenditure (in kilocalories). For the 6 training sessions, mice ran on a 0° incline for 2 min at 5 m/min, 5 min at 8 m/min, 5 min at 12 m/min, and then 20 min at 15 m/min, all of which is submaximal effort compared to VO_2 max testing.

Muscle Histology and Serum CK Assays

Mice were sacrificed 24 h following the final VO_2 max test. Quadriceps, gastrocnemius, tibialis anterior, diaphragm muscles, and hearts were flash frozen in -140°C isopentane. Muscles were sectioned on a cryostat (10- μm sections) and, prior to staining, sections were fixed for 10 min in 4% paraformaldehyde and then stained with H&E to quantify total fibers, central nuclei, and cross-sectional area. When

quantifying nuclei, no empty spaces were included in the field of view, as it was filled with muscle tissue, allowing us to normalize nuclei counts to the field rather than to a specific area. Fiber and central nuclei counts were obtained using Adobe Photoshop, while the cross-sectional area was obtained using ImageJ. Blood was collected via cardiac puncture, and clots were allowed to form while samples rested on ice. Samples were then centrifuged at 10,000 rpm for 10 min, and serum was collected. CK levels were then quantified using a colorimetric assay (Abcam) following the manufacturer's instructions.

Statistical Analysis

Statistical analyses were performed using Prism (GraphPad Software; La Jolla, CA, USA). Significant differences were determined using a normal or repeated-measures ANOVA (one- or two-way) as needed. Tukey's test for multiple mean comparisons was then used to identify differences between means. Values are presented as mean \pm SEM, and significance was accepted at $p \leq 0.05$. In the figures, differences between means are often indicated by different letters as defined in the legends. These definitions often differ between figures and panels (e.g., different letters signify a difference, each letter represents a specific comparison, etc.).

AUTHOR CONTRIBUTIONS

Conceptualization, J.W.M. and B.D.R.; Methodology, B.D.R., J.W.M., Y.B., D.K., and J.N.R.; Investigation, J.W.M., Y.B., and D.K.; Formal Analysis, B.D.R. and J.W.M.; Writing – Original Draft, B.D.R.; Writing – Review & Editing, B.D.R., J.W.M., and J.N.R.; Visualization, B.D.R., J.W.M., and Y.B.; Supervision, B.D.R.

CONFLICTS OF INTEREST

B.D.R. is the founder and CEO of AAVogen, which makes gene therapeutics for muscle wasting diseases. J.N.R. is a co-inventor of patents involving the micro-dystrophin gene therapeutics described herein. The other authors declare no competing interests.

ACKNOWLEDGMENTS

We thank the Viral Vector Core of the Seattle Wellstone Muscular Dystrophy Research Center for providing AAV vectors (NIH P50AR065139). This work was supported by grants to B.D.R. from the LGMD2I Research Fund and from the National Institutes of Health (R44CA221539). J.N.R. was also supported in part by a National Institutes of Health training grant (T32 GM007270).

REFERENCES

- Michele, D.E., and Campbell, K.P. (2003). Dystrophin-glycoprotein complex: post-translational processing and dystroglycan function. *J. Biol. Chem.* 278, 15457–15460.
- Wheeler, M.T., Allikian, M.J., Heydemann, A., and McNally, E.M. (2002). The sarcoglycan complex in striated and vascular smooth muscle. *Cold Spring Harb. Symp. Quant. Biol.* 67, 389–397.
- Roberts, R.G., Gardner, R.J., and Bobrow, M. (1994). Searching for the 1 in 2,400,000: a review of dystrophin gene point mutations. *Hum. Mutat.* 4, 1–11.
- Romitti, P.A., Zhu, Y., Puzhankara, S., James, K.A., Nabukera, S.K., Zamba, G.K., Ciafaloni, E., Cunniff, C., Druschel, C.M., Mathews, K.D., et al.; MD STARnet

- (2015). Prevalence of Duchenne and Becker muscular dystrophies in the United States. *Pediatrics* 135, 513–521.
5. Duan, D. (2018). Systemic AAV micro-dystrophin gene therapy for Duchenne muscular dystrophy. *Mol. Ther.* 26, 2337–2356.
 6. Chamberlain, J.R., and Chamberlain, J.S. (2017). Progress toward gene therapy for Duchenne muscular dystrophy. *Mol. Ther.* 25, 1125–1131.
 7. Dong, B., Nakai, H., and Xiao, W. (2010). Characterization of genome integrity for oversized recombinant AAV vector. *Mol. Ther.* 18, 87–92.
 8. Lai, Y., Yue, Y., and Duan, D. (2010). Evidence for the failure of adeno-associated virus serotype 5 to package a viral genome > or = 8.2 kb. *Mol. Ther.* 18, 75–79.
 9. Gao, Q.Q., and McNally, E.M. (2015). The dystrophin complex: structure, function, and implications for therapy. *Compr. Physiol.* 5, 1223–1239.
 10. Ervasti, J.M. (2007). Dystrophin, its interactions with other proteins, and implications for muscular dystrophy. *Biochim. Biophys. Acta* 1772, 108–117.
 11. Ramos, J.N., Hollinger, K., Bengtsson, N.E., Allen, J.M., Hauschka, S.D., and Chamberlain, J.S. (2019). Development of novel micro-dystrophins with enhanced functionality. *Mol. Ther.* 27, 623–635.
 12. Lai, Y., Thomas, G.D., Yue, Y., Yang, H.T., Li, D., Long, C., Judge, L., Bostick, B., Chamberlain, J.S., Terjung, R.L., and Duan, D. (2009). Dystrophins carrying spectrin-like repeats 16 and 17 anchor nNOS to the sarcolemma and enhance exercise performance in a mouse model of muscular dystrophy. *J. Clin. Invest.* 119, 624–635.
 13. Lai, Y., Zhao, J., Yue, Y., and Duan, D. (2013). $\alpha 2$ and $\alpha 3$ helices of dystrophin R16 and R17 frame a microdomain in the $\alpha 1$ helix of dystrophin R17 for neuronal NOS binding. *Proc. Natl. Acad. Sci. USA* 110, 525–530.
 14. Adams, M.E., Odom, G.L., Kim, M.J., Chamberlain, J.S., and Froehner, S.C. (2018). Syntrophin binds directly to multiple spectrin-like repeats in dystrophin and mediates binding of nNOS to repeats 16–17. *Hum. Mol. Genet.* 27, 2978–2985.
 15. Banks, G.B., Judge, L.M., Allen, J.M., and Chamberlain, J.S. (2010). The polyproline site in hinge 2 influences the functional capacity of truncated dystrophins. *PLoS Genet.* 6, e1000958.
 16. Banks, G.B., Combs, A.C., Chamberlain, J.R., and Chamberlain, J.S. (2008). Molecular and cellular adaptations to chronic myotendinous strain injury in mdx mice expressing a truncated dystrophin. *Hum. Mol. Genet.* 17, 3975–3986.
 17. De Luca, A., Pierno, S., Liantonio, A., Cetrone, M., Camerino, C., Fraysse, B., Mirabella, M., Servidei, S., Rüegg, U.T., and Conte Camerino, D. (2003). Enhanced dystrophic progression in mdx mice by exercise and beneficial effects of taurine and insulin-like growth factor-1. *J. Pharmacol. Exp. Ther.* 304, 453–463.
 18. Lefaucheur, J.P., Pastoret, C., and Sebille, A. (1995). Phenotype of dystrophinopathy in old mdx mice. *Anat. Rec.* 242, 70–76.
 19. Lynch, G.S., Hinkle, R.T., Chamberlain, J.S., Brooks, S.V., and Faulkner, J.A. (2001). Force and power output of fast and slow skeletal muscles from mdx mice 6–28 months old. *J. Physiol.* 535, 591–600.
 20. Rocco, A.B., Levalley, J.C., Eldridge, J.A., Marsh, S.A., and Rodgers, B.D. (2014). A novel protocol for assessing exercise performance and dystropathophysiology in the mdx mouse. *Muscle Nerve* 50, 541–548.
 21. Stuckey, D.J., Carr, C.A., Camelliti, P., Tyler, D.J., Davies, K.E., and Clarke, K. (2012). In vivo MRI characterization of progressive cardiac dysfunction in the mdx mouse model of muscular dystrophy. *PLoS ONE* 7, e28569.
 22. Gregorevic, P., Blankinship, M.J., Allen, J.M., and Chamberlain, J.S. (2008). Systemic microdystrophin gene delivery improves skeletal muscle structure and function in old dystrophic mdx mice. *Mol. Ther.* 16, 657–664.
 23. Bostick, B., Shin, J.H., Yue, Y., and Duan, D. (2011). AAV-microdystrophin therapy improves cardiac performance in aged female mdx mice. *Mol. Ther.* 19, 1826–1832.
 24. Bostick, B., Shin, J.H., Yue, Y., Wasala, N.B., Lai, Y., and Duan, D. (2012). AAV micro-dystrophin gene therapy alleviates stress-induced cardiac death but not myocardial fibrosis in >21-month-old mdx mice, an end-stage model of Duchenne muscular dystrophy cardiomyopathy. *J. Mol. Cell. Cardiol.* 53, 217–222.
 25. Bostick, B., Yue, Y., Long, C., Marschalk, N., Fine, D.M., Chen, J., and Duan, D. (2009). Cardiac expression of a mini-dystrophin that normalizes skeletal muscle force only partially restores heart function in aged mdx mice. *Mol. Ther.* 17, 253–261.
 26. Hoydal, M.A., Wisloff, U., Kemi, O.J., and Ellingsen, O. (2007). Running speed and maximal oxygen uptake in rats and mice: practical implications for exercise training. *Eur. J. Cardiovasc. Prev. Rehabil* 14, 753–760.
 27. Hafstad, A.D., Boardman, N.T., Lund, J., Hagve, M., Khalid, A.M., Wisloff, U., Larsen, T.S., and Aasum, E. (2011). High intensity interval training alters substrate utilization and reduces oxygen consumption in the heart. *J. Appl. Physiol.* 111, 1235–1241.
 28. Maricelli, J.W., Kagel, D.R., Bishaw, Y.M., Nelson, O.L., Lin, D.C., and Rodgers, B.D. (2017). Sexually dimorphic skeletal muscle and cardiac dysfunction in a mouse model of limb girdle muscular dystrophy 2i. *J. Appl. Physiol.* (1985) 123, 1126–1138.
 29. Burdi, R., Rolland, J.F., Fraysse, B., Litvinova, K., Cozzoli, A., Giannuzzi, V., Liantonio, A., Camerino, G.M., Sblendorio, V., Capogrosso, R.F., et al. (2009). Multiple pathological events in exercised dystrophic mdx mice are targeted by pentoxifylline: outcome of a large array of in vivo and ex vivo tests. *J. Appl. Physiol.* 106, 1311–1324.
 30. De Luca, A., Nico, B., Rolland, J.F., Cozzoli, A., Burdi, R., Mangieri, D., Giannuzzi, V., Liantonio, A., Cippone, V., De Bellis, M., et al. (2008). Gentamicin treatment in exercised mdx mice: Identification of dystrophin-sensitive pathways and evaluation of efficacy in work-loaded dystrophic muscle. *Neurobiol. Dis.* 32, 243–253.
 31. De Luca, A., Pierno, S., Liantonio, A., and Conte Camerino, D. (2002). Pre-clinical trials in Duchenne dystrophy: what animal models can tell us about potential drug effectiveness. *Neuromuscul. Disord.* 12 (Suppl 1), S142–S146.
 32. Nagaraju, K., and Willmann, R.; TREAT-NMD Network and the Wellstone Muscular Dystrophy Cooperative Research Network (2009). Developing standard procedures for murine and canine efficacy studies of DMD therapeutics: report of two expert workshops on “Pre-clinical testing for Duchenne dystrophy”: Washington DC, October 27th–28th 2007 and Zürich, June 30th–July 1st 2008. *Neuromuscul. Disord.* 19, 502–506.
 33. Rodgers, B.D., Eldridge, J.A., and Marsh, S.A. (2014). Use of Respiratory and Exercise Performance to Quantify Systemic Muscle Function in mdx Mice (TREAT-NMD Neuromuscular Network).
 34. Spurney, C.F., Gordish-Dressman, H., Guerron, A.D., Sali, A., Pandey, G.S., Rawat, R., Van Der Meulen, J.H., Cha, H.J., Pistilli, E.E., Partridge, T.A., et al. (2009). Preclinical drug trials in the mdx mouse: assessment of reliable and sensitive outcome measures. *Muscle Nerve* 39, 591–602.
 35. Grounds, M.D., Radley, H.G., Lynch, G.S., Nagaraju, K., and De Luca, A. (2008). Towards developing standard operating procedures for pre-clinical testing in the mdx mouse model of Duchenne muscular dystrophy. *Neurobiol. Dis.* 31, 1–19.
 36. Bostick, B., Yue, Y., Lai, Y., Long, C., Li, D., and Duan, D. (2008). Adeno-associated virus serotype-9 microdystrophin gene therapy ameliorates electrocardiographic abnormalities in mdx mice. *Hum. Gene Ther.* 19, 851–856.
 37. Wasala, N.B., Shin, J.H., Lai, Y., Yue, Y., Montanaro, F., and Duan, D. (2018). Cardiac-specific expression of Δ H2-R15 mini-dystrophin normalized all electrocardiogram abnormalities and the end-diastolic volume in a 23-month-old mouse model of Duchenne dilated cardiomyopathy. *Hum. Gene Ther.* 29, 737–748.
 38. Abmayr, S., Gregorevic, P., Allen, J.M., and Chamberlain, J.S. (2005). Phenotypic improvement of dystrophic muscles by rAAV/microdystrophin vectors is augmented by Igf1 codelivery. *Mol. Ther.* 12, 441–450.
 39. Gregorevic, P., Plant, D.R., Leeding, K.S., Bach, L.A., and Lynch, G.S. (2002). Improved contractile function of the mdx dystrophic mouse diaphragm muscle after insulin-like growth factor-I administration. *Am. J. Pathol.* 161, 2263–2272.
 40. Rodino-Klapac, L.R., Janssen, P.M., Shontz, K.M., Canan, B., Montgomery, C.L., Griffin, D., Heller, K., Schmelzer, L., Handy, C., Clark, K.R., et al. (2013). Micro-dystrophin and follistatin co-delivery restores muscle function in aged DMD model. *Hum. Mol. Genet.* 22, 4929–4937.
 41. Mendell, J.R., Sahenk, Z., Malik, V., Gomez, A.M., Flanigan, K.M., Lowes, L.P., Alfano, L.N., Berry, K., Meadows, E., Lewis, S., et al. (2015). A phase 1/2a follistatin gene therapy trial for becker muscular dystrophy. *Mol. Ther.* 23, 192–201.
 42. Schneyer, A.L., Sidis, Y., Gulati, A., Sun, J.L., Keutmann, H., and Krasney, P.A. (2008). Differential antagonism of activin, myostatin and growth and differentiation factor 11 by wild-type and mutant follistatin. *Endocrinology* 149, 4589–4595.
 43. Benabdallah, B.F., Bouchentouf, M., Rousseau, J., Bigey, P., Michaud, A., Chapdelaine, P., Scherman, D., and Tremblay, J.P. (2008). Inhibiting myostatin

- with follistatin improves the success of myoblast transplantation in dystrophic mice. *Cell Transplant.* 17, 337–350.
44. Benabdallah, B.F., Bouchentouf, M., and Tremblay, J.P. (2005). Improved success of myoblast transplantation in mdx mice by blocking the myostatin signal. *Transplantation* 79, 1696–1702.
 45. Byron, C.D., Hamrick, M.W., and Wingard, C.J. (2006). Alterations of temporalis muscle contractile force and histological content from the myostatin and Mdx deficient mouse. *Arch. Oral Biol.* 51, 396–405.
 46. Hulmi, J.J., Oliveira, B.M., Silvennoinen, M., Hoogaars, W.M., Ma, H., Pierre, P., Pasternack, A., Kainulainen, H., and Ritvos, O. (2013). Muscle protein synthesis, mTORC1/MAPK/Hippo signaling, and capillary density are altered by blocking of myostatin and activins. *Am. J. Physiol. Endocrinol. Metab.* 304, E41–E50.
 47. Morine, K.J., Bish, L.T., Selsby, J.T., Gazzara, J.A., Pendrak, K., Sleeper, M.M., Barton, E.R., Lee, S.J., and Sweeney, H.L. (2010). Activin IIB receptor blockade attenuates dystrophic pathology in a mouse model of Duchenne muscular dystrophy. *Muscle Nerve* 42, 722–730.
 48. Wagner, K.R., McPherron, A.C., Winik, N., and Lee, S.J. (2002). Loss of myostatin attenuates severity of muscular dystrophy in mdx mice. *Ann. Neurol.* 52, 832–836.
 49. National Institutes of Health. *ClinicalTrials.gov*. <https://clinicaltrials.gov/ct2/results?term=ace-031>.
 50. Plumridge, H., and Falconi, M. (2014). Drugs aim to help elderly rebuild muscle. *Wall Street Journal*, April 27, 2014. <https://www.wsj.com/articles/drugs-aims-to-help-elderly-rebuild-muscle-1398644791>.
 51. Garber, K. (2016). No longer going to waste. *Nat. Biotechnol.* 34, 458–461.
 52. Maricelli, J.W., Bishaw, Y.M., Wang, B., Du, M., and Rodgers, B.D. (2018). Systemic Smad7 gene therapy increases striated muscle mass and enhances exercise capacity in a dose-dependent manner. *Hum. Gene Ther.* 29, 390–399.
 53. Winbanks, C.E., Murphy, K.T., Bernardo, B.C., Qian, H., Liu, Y., Sepulveda, P.V., Beyer, C., Hagg, A., Thomson, R.E., Chen, J.L., et al. (2016). Smad7 gene delivery prevents muscle wasting associated with cancer cachexia in mice. *Sci. Transl. Med.* 8, 348ra98.
 54. Hakim, C.H., Wasala, N.B., Pan, X., Kodippili, K., Yue, Y., Zhang, K., Yao, G., Haffner, B., Duan, S.X., Ramos, J., et al. (2017). A five-repeat micro-dystrophin gene ameliorated dystrophic phenotype in the severe DBA/2J-mdx model of Duchenne muscular dystrophy. *Mol. Ther. Methods Clin. Dev.* 6, 216–230.
 55. Hilton, T., Orr, R.D., Perkin, R.M., and Ashwal, S. (1993). End of life care in Duchenne muscular dystrophy. *Pediatr. Neurol.* 9, 165–177.
 56. Van Ruiten, H.J., Marini Bettolo, C., Cheetham, T., Eagle, M., Lochmuller, H., Straub, V., Bushby, K., and Guglieri, M. (2016). Why are some patients with Duchenne muscular dystrophy dying young: an analysis of causes of death in North East England. *Eur. J. Paediatr. Neurol.* 20, 904–909.
 57. Bassett, D.R., Jr., and Howley, E.T. (2000). Limiting factors for maximum oxygen uptake and determinants of endurance performance. *Med. Sci. Sports Exerc.* 32, 70–84.
 58. Ciafaloni, E., Fox, D.J., Pandya, S., Westfield, C.P., Puzhankara, S., Romitti, P.A., Mathews, K.D., Miller, T.M., Matthews, D.J., Miller, L.A., et al. (2009). Delayed diagnosis in Duchenne muscular dystrophy: data from the Muscular Dystrophy Surveillance, Tracking, and Research Network (MD STARnet). *J. Pediatr.* 155, 380–385.
 59. Mohamed, K., Appleton, R., and Nicolaides, P. (2000). Delayed diagnosis of Duchenne muscular dystrophy. *Eur. J. Paediatr. Neurol.* 4, 219–223.
 60. Wong, S.H., McClaren, B.J., Archibald, A.D., Weeks, A., Langmaid, T., Ryan, M.M., Kornberg, A., and Metcalfe, S.A. (2015). A mixed methods study of age at diagnosis and diagnostic odyssey for Duchenne muscular dystrophy. *Eur. J. Hum. Genet.* 23, 1294–1300.
 61. Salva, M.Z., Himeda, C.L., Tai, P.W., Nishiuchi, E., Gregorevic, P., Allen, J.M., Finn, E.E., Nguyen, Q.G., Blankinship, M.J., Meuse, L., et al. (2007). Design of tissue-specific regulatory cassettes for high-level rAAV-mediated expression in skeletal and cardiac muscle. *Mol. Ther.* 15, 320–329.
 62. Himeda, C.L., Chen, X., and Hauschka, S.D. (2011). Design and testing of regulatory cassettes for optimal activity in skeletal and cardiac muscles. *Methods Mol. Biol.* 709, 3–19.
 63. Gonçalves, M.A., Janssen, J.M., Nguyen, Q.G., Athanasopoulos, T., Hauschka, S.D., Dickson, G., and de Vries, A.A. (2011). Transcription factor rational design improves directed differentiation of human mesenchymal stem cells into skeletal myocytes. *Mol. Ther.* 19, 1331–1341.
 64. Martari, M., Sagazio, A., Mohamadi, A., Nguyen, Q., Hauschka, S.D., Kim, E., and Salvatori, R. (2009). Partial rescue of growth failure in growth hormone (GH)-deficient mice by a single injection of a double-stranded adeno-associated viral vector expressing the GH gene driven by a muscle-specific regulatory cassette. *Hum. Gene Ther.* 20, 759–766.
 65. Bengtsson, N.E., Seto, J.T., Hall, J.K., Chamberlain, J.S., and Odom, G.L. (2016). Progress and prospects of gene therapy clinical trials for the muscular dystrophies. *Hum. Mol. Genet.* 25 (R1), R9–R17.
 66. Hu, C., Kasten, J., Park, H., Bhargava, R., Tai, D.S., Grody, W.W., Nguyen, Q.G., Hauschka, S.D., Cederbaum, S.D., and Lipshutz, G.S. (2014). Myocyte-mediated arginase expression controls hyperargininemia but not hyperammonemia in arginase-deficient mice. *Mol. Ther.* 22, 1792–1802.
 67. Muir, L.A., Nguyen, Q.G., Hauschka, S.D., and Chamberlain, J.S. (2014). Engraftment potential of dermal fibroblasts following in vivo myogenic conversion in immunocompetent dystrophic skeletal muscle. *Mol. Ther. Methods Clin. Dev.* 1, 14025.
 68. Le Rumeur, E., Winder, S.J., and Hubert, J.F. (2010). Dystrophin: more than just the sum of its parts. *Biochim. Biophys. Acta* 1804, 1713–1722.